Journal of Membrane Science 609 (2020) 118189

Contents lists available at ScienceDirect

Journal of Membrane Science

journal homepage: http://www.elsevier.com/locate/memsci

A comparison between chemical cleaning efficiency in lab-scale and full-scale reverse osmosis membranes: Role of extracellular polymeric substances (EPS)

M. Jafari [a,b,*], A. D'haese [b], J. Zlopasa [a], E.R. Cornelissen [b,c,d], J.S. Vrouwenvelder [a,e], K. Verbeken [f], A. Verliefde [b], M.C.M. van Loosdrecht [a], C. Picioreanu [a]

[a] Department of Biotechnology, Faculty of Applied Sciences, Delft University of Technology, Van der Maasweg 9, 2629 HZ, Delft, the Netherlands
[b] Particle and Interfacial Technologies Group, Faculty of Bioscience Engineering, Ghent University, Coupure Links 653, B-9000, Ghent, Belgium
[c] KWR Water Cycle Research Institute, Groningenhaven 7, 3433 PE, Nieuwegein, the Netherlands
[d] Singapore Membrane Technology Centre, Nanyang Environment and Water Research Institute, Nanyang Technological University, Singapore, 637141, Singapore
[e] King Abdullah University of Science and Technology (KAUST), Water Desalination and Reuse Center (WDRC), Division of Biological and Environmental Science and Engineering (BESE), Thuwal, 23955-6900, Saudi Arabia
[f] Department of Materials, Textiles and Chemical Engineering, Ghent University, Technologiepark Zwijnaarde 46, B-9052, Zwijnaarde, Belgium

ARTICLE INFO

Keywords:
Chemical cleaning efficiency
Extracellular polymeric substances (EPS)
EPS composition
EPS adherence
Desalination

ABSTRACT

Chemical cleaning is vital for the optimal operation of membrane systems. Membrane chemical cleaning protocols are often developed in the laboratory flow cells (e.g., Membrane Fouling Simulator (MFS)) using synthetic feed water (nutrient excess) and short experimental time of typically days. However, full-scale Reverse Osmosis (RO) membranes are usually fed with nutrient limited feed water (due to extensive pre-treatment) and operated for a long-time of typically years. These operational differences lead to significant differences in the efficiency of chemical Cleaning-In-Place (CIP) carried out on laboratory-scale and on full-scale RO systems. Therefore, we investigated the suitability of lab-scale CIP results for full-scale applications. A lab-scale flow cell (i.e., MFSs) and two full-scale RO modules were analysed to compare CIP efficiency in terms of water flux recovery and biofouling properties (biomass content, Extracellular Polymeric Substances (EPS) composition and EPS adherence) under typical lab-scale and full-scale conditions. We observed a significant difference between the CIP efficiency in lab-scale (~50%) and full-scale (9–20%) RO membranes. Typical biomass analysis such as Total Organic Carbon (TOC) and Adenosine triphosphate (ATP) measurements did not indicate any correlation to the observed trend in the CIP efficiency in the lab-scale and full-scale RO membranes. However, the biofilms formed in the lab-scale contains different EPS than the biofilms in the full-scale RO modules. The biofilms in the lab-scale MFS have polysaccharide-rich EPS (Protein/Polysaccharide ratio = 0.5) as opposed to biofilm developed in full-scale modules which contain protein-rich EPS (Protein/Polysaccharide ratio = 2.2). Moreover, EPS analysis indicates the EPS extracted from full-scale biofilms have a higher affinity and rigidity to the membrane surface compared to EPS from lab-scale biofilm. Thus, we propose that CIP protocols should be optimized in long-term experiments using the realistic feed water.

1. Introduction

Biofouling is an undesired accumulation of microorganisms on surfaces due to the deposition of organic compounds and/or growth of microorganisms (biofilm formation) [1,2]. Biofouling adversely impacts membrane filtration systems by causing an additional hydraulic resistance [3,4], reduction in apparent membrane permeability and selectivity [5,6], and higher feed channel pressure drop [2,7,8]. Physical and chemical cleaning routines are periodically applied to reduce biofouling impacts on membrane systems. Physical cleaning is applied frequently in membrane systems (i.e., UF, MF) using different approaches such as back-wash cleaning [9], shear cleaning [10,11] and

* Corresponding author. Department of Biotechnology, Faculty of Applied Sciences, Delft University of Technology, Van der Maasweg 9, 2629 HZ, Delft, the Netherlands.
E-mail address: m.jafarieshlaghi@tudelft.nl (M. Jafari).

https://doi.org/10.1016/j.memsci.2020.118189
Received 17 January 2020; Received in revised form 10 April 2020; Accepted 12 April 2020
Available online 4 May 2020

air-bubble cleaning [12]. Chemical cleaning protocols include chemically-enhanced backwash and Cleaning-In-Place (CIP) typically using acid and base solutions. The goal of both physical and chemical cleanings is to remove foulants and restore membrane performance as close as possible to virgin membranes. In dense membrane systems (RO, NF) in spiral wound configuration, hydraulic cleaning options are limited because the membranes cannot be backwashed.

The efficiency of CIP cleaning routines depends on type of cleaning solvents, solvent concentration, contact time, temperature and hydraulic parameters (kinetic or static cleaning) [13,14]. The CIP cleaning mechanisms can be concluded namely such as hydrolysis, solubilisation, dispersion and chelating [15]. Chemical agents such as acids, bases, surfactants, chelating agents, oxidizing agents, and enzymes are used in CIP cleaning of RO membranes [15]. Generally, acids (e.g., HCl) and bases (e.g., NaOH) are among the most popular chemical agents used in RO membranes thanks to their economic advantages. Acids are used to dissolves precipitate of inorganics salts while alkaline agents can promote protein and polysaccharide hydrolysis and weaken membrane-foulant bonds [13].

Although periodical CIP cleanings are vital for a stable membrane operation, CIP cleanings are only partially successful in the recovery of both water permeability and pressure drop [7,14–16]. Residual biofilm has been observed to remain on the membrane surface even after several cycles of CIP cleanings, leading to biofilm regrowth [17]. The membranes cleaned by CIP have a higher biofouling potential compared to the virgin membranes, due to nutrient availability resulting from the lysis of killed cells [18]. Chemical cleaning leads to changes in biofouling layer properties such as microbial community composition and extracellular polymeric substances (EPS) properties. Al Ashhab et al. [19] suggested that several rounds of CIP in reverse osmosis (RO) membranes leads to formation of biofilms with limited microbial diversity and higher adherence to the membrane surface.

Novel CIP protocols (e.g. biocides, chelating agents and enzymes) already demonstrated superior recoveries of water permeability and feed channel pressure drop [16,20,21]. Often, the novel CIP routines enhance EPS solubilisation leading to more effective and long-term biomass removal by higher degree of protein denaturation [16]. Often, these CIP protocols are developed and optimized in the lab conditions using Membrane Fouling Simulator (MFS) [8,14,16,21–26]. MFS is widely used in fouling and CIP studies due to its similarity in hydrodynamics to spiral wound RO membranes as well as its practicality in terms of low amount of water and chemicals required [27].

The EPS, forming the biofilm matrix, play a distinctive role in biofouling cleanability in membrane processes. The EPS from biofilms developed on membrane surfaces (i.e. membrane biofilm EPS) are evaluated based on their main composition (i.e., polysaccharide, protein) and adherence properties to the membrane surface [19,28]. Herzberg et al. [6] reported EPS with high concentration of polysaccharide for biofilms developed in lab RO flow cells using synthetic wastewater. Similarly, the EPS extracted from the biofilms grown in the MFS has a protein/polysaccharide ratio of around 0.5 (i.e., polysaccharide-rich EPS) [16]. Desmond et al. [29] reported that the protein/polysaccharide ratio in EPS increases with the biofilm age in a dead-end UF system fed with synthetic wastewater. A similar trend was observed with increasing Solid Retention Time (SRT) in a lab-scale Membrane Bioreactor (MBR) [28]. Bucs et al. [30] reported that amphiphilic coating of reverse osmosis membrane would increase the formation of protein-rich EPS on the membrane surface. Al Ashhab et al. [19] studied the EPS properties (composition, adherence) for biofilms grown in lab-scale RO systems subjected to several rounds of CIP and they reported a polysaccharide-rich EPS. Recently, Farhat et al. [8] observed that a protein-rich EPS is formed for the biofilms growing under phosphate limitation. However, Beyer et al. [15] measured the EPS composition for three full-scale RO installations and they reported polysaccharide-rich EPS from biofilms developed in full-scale RO plants. It is therefore apparent that the EPS composition depends on the biofilm age, nutrient availability in the feed water, and membrane surface properties.

The studies of EPS from membrane biofilms have been mainly focused on biofouling developed in lab conditions (typically, fast grown biofilms), usually fed with synthetic feed water for short periods of time [6,17–19]. However, EPS properties of biofilms developed in full-scale installations (i.e., "old" biofilms and under nutrient limitation) are not well explored, probably due to time limitations, sampling difficulty, and diversity in plant operational conditions. Surprisingly, researchers reported significantly different results for the lab-scale CIP cleaning efficiency compared to full-scale plants [31].

The aim of this study was to evaluate the applicability of CIP results from typical lab-scale MFS to full-scale RO plants. Therefore, we investigated i) the difference between biofilm removal and water flux recovery after conventional chemical cleaning of full-scale modules and lab-scale MFSs, and ii) the difference in EPS properties (i.e., composition and, adherence) for biofilms formed in full-scale RO modules and lab-scale MFSs. These objectives allow for a better understanding of the correlation between the CIP efficiency and the properties of EPS in biofilms formed in membrane processes.

2. Materials and methods

2.1. Experimental set-up and fouling protocol

Laboratory set-up for "natural biofouling" growth in a MFS includes a feed pump, nutrient pump, level controller, pressure safety valve, bypass valve, mass flow meter, back pressure valve, and a MFS [24]. A back-pressure valve was installed to prevent degassing by pressurizing the set-up. A MFS with flow channel dimensions of 250 × 50 × 1 mm and a membrane with active area of 124.14 cm^2 were used. The RO membrane used in the MFS was provided by DOW FILMTEC (Table 1). The MFS was operated under transmembrane pressure TMP = 2 bar and in cross-flow mode with linear velocity of 0.15 m/s, representative of

Table 1
Feed water characteristics and operational conditions of the MFS and the full-scale plants in Belgium (Plant A) and in The Netherlands (Plant B).

Case studies	MFS	Plant A	Plant B
Membrane properties and operational condition			
Location	Ghent, Belgium	Veurne, Belgium	Zuid-Holland, Netherlands
Manufacturer	DOW FILMTEC	Toray	DOW FILMTEC
Membrane elements	XLE BW30	TM720D-400	ECO-PRO 440-i
Water permeability[a] (L/m^2/h/bar)	7.49 ± 0.77	3.01	4.7
Salt rejection	~97%	90.3%	99.4%
Operational time	20 days	2 years	1.5 years
Historical CIP protocol	N.A.	Caustic/Citric acid[b]	Hydrochloric acid/ Caustic[c]
Days since last CIP	N.A.	35 days	60 days
Feed water characteristics			
Type of feed water	Tap water	Industrial effluent	Surface water
TOC (mg/L)	<0.2	7 ± 0.3	4.3 ± 0.06
pH	7.5	6.5	9.3
Total Hardness (mmol/L)	1.2	4.9	0.06
Conductivity (μS/cm)	453	3140	547

[a] Virgin membrane permeability based on supplier data.
[b] The CIP protocol of Plant A consists of four steps: 1) NaOH (pH 12) at 20–32 °C for 4 h, 2) rinsing with permeate water, 3) Citric acid (pH 2.5–3) at 20–32 °C for 2 h and followed by the final rinsing with permeate water. This protocol "Historical CIP" is only practiced during full-scale operation.
[c] The CIP protocol of Plant B consists of four steps: 1) HCl (pH 2) at 5–25 °C for 2 h, 2) rinsing with demineralized water, 3) NaOH (pH 12) at 40 °C for 2 h and followed by the final rinsing with demineralized water. This protocol is only practiced during full-scale operation.

practical operation [32]. Such MFS operation (i.e., at TMP ~ 1–6 bar) has been vastly reported for studies of model fouling development and membrane cleaning (e.g, CIP) in RO processes [8,16,24–26,31]. The MFS retentate was partially recirculated (200 mL/min equivalent of 75% of feed flow rate) to ensure the availability of fresh tap water in the feed storage. Tap water in city of Ghent, Belgium, with minimal residual chlorine was used as feed water for "natural biofouling" growth (no inoculation). Feed water characteristic are listed in Table 1.

Biofilm development in the MFS was accelerated by dosing a nutrient solution containing sodium acetate, sodium nitrate and sodium dihydrogen phosphate in a mass ratio C:N:P of 100:20:10 to the feed water [24]. The phosphate concentration was considered in excess to prevent the risk of phosphate limitation (which can be applied as a biofouling control strategy). The concentration of acetate added to the feed water was 1 mg/L [16,24]. During operation, the MFS was covered to prevent any growth of phototropic microorganisms. The nutrient stock solution was replaced every 2 days. The nutrient solution was dosed using a calibrated peristaltic pump with the flow rate of 0.03 L/h. The nutrient flow rate was set much lower than feed flow rate to ensure the effect of nutrient dosage on feed solution pH is negligible [16,25]. As previously reported by Vrouwenvelder et al. [27] the MFS test-rig installed in parallel to full-scale RO (identical feed water) delivered comparable results (i.e., feed channel pressure drop) for spiral-wound RO and MFS. However, due to practical considerations, fouling studies and CIP protocol developments are often carried out in lab conditions (e.g., synthetic feed water, short-term) [8,16,24–26,31]. The MFS operational conditions in current study have been selected based on the rationale that such conditions are widely reported in the literature, thus, the results can be compared to existing data.

2.2. Full-scale membrane modules autopsy

Two full-scale Reverse Osmosis (RO) installations in Belgium (Plant A) and in The Netherlands (Plant B) which both are operating at constant flux using surface water as feed water were studied. The feed water characteristics of the full scale plants are listed in Table 1.

Plant A is a water reuse plant for a potato chips and snack factory (PepsiCo) in Veurne, Belgium. The installation consists of ultrafiltration (UF) as a pre-treatment and a one-stage RO as a main purification step. The Plant B is a demineralized water production plant in Rotterdam, The Netherlands, providing a demineralized water to a broad range of industries in the Rotterdam harbour area. Pre-treatment steps at Plant B include a Dissolved Air Flotation sand Filtration (DAFF), Water softener and two-stages RO (as the main purification steps). The post-treatment consists of a mixed-bed ion exchange resins to remove the residual ions. Periodical CIP was performed in both full-scale plants as the feed channel pressure increased by 20%. From each full-scale installation, one membrane element (lead module) was taken and opened for autopsy.

Membrane modules were transported for autopsy within 3 h of extraction from the pressure vessels. Membrane modules were refrigerated at 7 °C. Biofouling samples were taken from membrane sheets randomly (at least 3 locations along the module). The samples size vary between 10 and 30 cm^2. The results of all the analysis were normalized by samples area for further comparative assessment.

2.3. Water permeability and chemical cleaning

Water flux was measured to evaluate membrane performance before and after CIP. Water permeability [L/m^2/h/bar] ($\frac{Flux[Lm^{-2}h^{-1}]}{TMP[bar]}$) and CIP recovery [%] ($\frac{Flux_{afterCIP}-Flux_{beforeCIP}}{Flux_{beforeCIP}}$) were calculated before and after CIP to investigate water permeability recovery by such a cleaning. To determine the water permeability, membrane samples (i.e., membrane sheet and feed spacer) which were cut from the membrane modules and the MFS were placed in a high pressure flow cell with identical dimensions as mentioned above. Water permeability measurements were carried out using deionized water under transmembrane pressure of 5 bar in the cross-flow mode (with cross flow velocity 0.15 m/s, from practice). Water flux/permeability measurements were carried out in duplicate before and after CIP. Water permeability data were recorded at least 15 min after stable water flux was recorded.

A conventional chemical cleaning was applied in both MFS and full-scale modules which includes the following steps *i*) alkaline cleaning (NaOH, pH 12, 0.01 M, 35 °C, 1 h), *ii*) Rinsing with DI water for 15 min, *iii*) Acid cleaning (HCl, pH 1, 0.1 M, room temperature, 1 h), iv) final rinsing with DI water for 15 min. The chemical solutions were circulated with an identical flow rate as used for feed water [16].

2.4. Biomass quantification

The membrane sheets and spacers were cut to quantify biomass in lab-scale MFS and full-scale plants. Membrane and spacer samples were cut from membrane sheets and places in a centrifuge tube containing 30 mL sterile tap water for Adenosine triphosphate (ATP) measurements and in the ultrapure water for Total Organic Carbon (TOC) analysis. The centrifuge tubes with membrane samples were placed in an ultrasonic water bath (5510E-DTH, Bransonic, Danbury, CT) for 2 min and 1 min of vortex mixer to detach biofilm from membrane and spacer surfaces [8]. The procedure was repeated three times and the solution in the centrifuge tube was used to measure ATP and TOC. ATP measurements have been carried out to quantify the active biomass accumulated on both spacer and membrane surfaces before and after chemical cleaning. ATP is present in all viable microorganisms thus it is widely acceptable for biomass analysis [2,16,33]. TOC measurements were carried out to quantify total organic carbon contained in both biofilm cells and extracellular polymeric substances (EPS) [24].

2.5. EPS extraction and composition

To analyse the EPS composition and adherence properties, EPS was extracted from the accumulated biomass on the membrane. The membrane coupons were cut from membrane sheets. The EPS was extracted under alkaline conditions as previously described by Ref. [34]. The biofilm was initially treated with 0.1 NaOH for 30 min at 80 °C followed by centrifugation at 20,000×g, where the solid residue was separated from the supernatant that contains the soluble EPS.

Polysaccharide and protein contents in the EPS were qualified using colorimetric methods. Polysaccharides concentration was determined based on Dubois method [35] with glucose as the standard. Protein content was determined using Bio-Rad[a] Protein assay using Bovine serum albumin, BSA, as the standard [36].

2.6. EPS adherence properties using quartz crystal microbalance with dissipation (QCM-D)

To determine the adherence properties of EPS, the adsorption kinetics of EPS was measured using Quartz Crystal Microbalance and Dissipation, QCM-D, (Q-Sense E4, Gothenburg, Sweden). EPS adherence properties to a surface were characterized by measuring the change of oscillation frequency of the sensor. Generally, the QCM-D measurements determine the physical properties of the deposited film on the sensor surface. The adsorbed mass on the sensor (Δm) linearly correlated to the frequency change (ΔF) by Sauerbrey equation $\Delta m = -\frac{C}{n}\Delta F$ where c is the mass sensitivity constant (17.7 ng/cm2/Hz at F = 5 MHz) and n is the overtone number (1,2,3,..). Thus, the mass uptake on the sensor is linearly correlated with frequency changes [37]. The change in frequency could be related to both bulk liquid physical properties such as density and viscosity as well as the adsorbed layer mass on the sensor. Fig. 1 indicates an example of frequency results of QCM-D measurements subjected to pure water, salt and polymer solutions on both bare gold

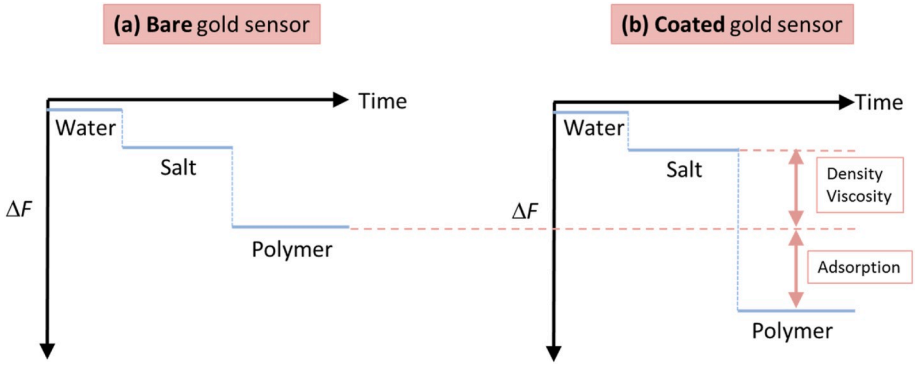

Fig. 1. An example of QCM-D measurements results of frequency shift over time for a) bare (uncoated) gold sensor and b) coated gold sensor (e.g., polyamide) in contact with water, salt solution, and polymer solution. The changes in frequency for bare gold sensor (assuming no adsorption) are only correlated to bulk liquid density and viscosity. However, for the coated sensor, the frequency shifts for polymer solution have adsorption contribution on top of effects of bulk liquid density and viscosity. (For interpretation of the references to color in this figure legend, the reader is referred to the Web version of this article.)

and coated sensors. Assuming no adsorption of salt and polymer to the gold sensor, the change in frequency of bare gold sensor is only caused by bulk liquid viscosity and density. However, due to interaction of polymer solution with the coated gold sensor (polymer-polymer interaction), the frequency shift in the coated gold sensor is even higher for the polymer solution compared to bare gold sensor (Fig. 1). This higher reduction in frequency of coated sensor is correlated to the adsorption of thin film of polymer on the coated sensor.

Moreover, the decay of crystal oscillation can be correlated to the energy dissipated in each oscillation. The dissipation factor in every oscillation circuit can be defined as $D = \frac{Energy\ \ dissipiated}{Energy\ \ stored\ \ in\ \ crystal}$. $\Delta D/\Delta F$ ratio provides information on how energy is dissipated per oscillation. A higher $\Delta D/\Delta F$ ratio is correlated to the non-rigid adsorbed layer as appose to low $\Delta D/\Delta F$ ratio which correspond to rigid adsorbed film [19].

The variations of frequency, F, and dissipation factor, D, were measured for the two overtones n = 5,7). EPS adherence properties (i.e., rigidity) on the crystal sensor was measured by analysing the correlation between the shift in frequency and dissipation factor of different EPS biofilms [19,28]. The QCM-D measurements were carried out on both on bare-gold sensor and sensor coated with polyamide (Nomex, Sigma-Aldrich) with fundamental resonant frequency of 5 MHz. The sensors were coated with polyamide to mimic the RO membrane surface [19,28]. Prior to experiments, the sensors were soaked in 5 mM ethylenediaminetetraacetic acid (EDTA) for 30 min followed by rinsing thoroughly with Milli-Q water and finally dried with pure N_2 as described by Sweity et al. [28]. A background solution containing 8.5 mM NaCl +0.5 mM$CaCl_2$ (background solution) was considered the standard solution. EPS solution was diluted into background solution to 5.5 mM of TOC (EPS standard solution). EPS aqueous solution flows above coated sensors at constant temperature of 22 °C and flowrate of 150 μL/min (cross-flow mode). At least two EPS samples were extracted from each membrane module [19]. The protocol reported by Al Ashhab et al. [19] was followed including three steps. i) 20 min Milli-Q water; ii) 20 min 10 mM background solution (8.5 mM NaCl + 0.5 mMCaCl2); iii) 30 min of 10 mM standard EPS solution (containing 5.5 mg/L TOC and diluted by background solution). An identical protocol was carried out on a bare gold sensor in order to subtract the impact of bulk viscosity and density of the frequency shift of the coated sensor.

2.7. Fouling layer morphology: scanning electron microscope (SEM) imaging

Morphological properties of the fouling layers were observed using Scanning Electron Microscopy (SEM). The dried fouled membrane samples were coated with gold for 30 s. Two different resolutions (500 and 10,000- fold magnifications) were applied to observe and compare the structural properties of different fouling layers [19,38]. The compositional details of fouling layers were characterized using energy dispersive X-ray (EDX).

3. Results

A lab-scale MFS and two full-scale RO modules were analysed to compare CIP efficiency (in terms of water flux recovery) and biofouling properties (biomass content and EPS properties) in the typical lab-scale and full-scale conditions. The operational characteristics of the MFS and full-scale RO modules are listed in Table 1.

3.1. Water permeability and CIP recovery

The water flux was measured for the virgin membrane, as well as for the fouled membranes before and after CIP cleaning. The water permeability was derived by normalizing water flux to the applied TMP. The water flux for the virgin membrane was measured to compare the impact of biofouling in water permeability decline. Fig. 2a shows water permeability for the lab-scale MFS and two full-scale RO modules. The water permeability decreased in the MFS from around 6 to 3 L/m^2/h/bar due to the fouling. Similarly, for the full-scale modules water permeability was reduced from around 3 to 1 L/m^2/h/bar for Plant A and from ~4.5 to 1.7 L/m^2/h/bar for Plant B. After CIP, the water permeability recovered significantly more in the MFS compared to the full-scale modules, increasing from ~3.0 to 4.5 L/m^2/h/bar for MFS while only from about 1 to 1.2 L/m^2/h/bar for plant A (Fig. 2a). Clearly, CIP was more effective in MFS (~50% recovery) compared to full-scale Plant A (~22%) and Plant B (~9%) (Fig. 2b). Such considerable difference in CIP recovery raises questions on the applicability of CIP results obtained in "typical" MFS experiments as an indication for full-scale plants.

3.2. Biomass quantification and chemical cleaning efficiency

To evaluate the relation between the water permeability recovery and the biomass accumulation, we measured the amount of biomass deposited on the membrane and the removal of biomass via CIP cleaning. Biomass accumulated on the membrane surface was quantified using typical ATP and TOC measurements before and after chemical cleaning. Fig. 3a shows ATP concentration in the MFS and two full-scale modules. ATP concentration before cleaning for the MFS is around 1000 pg/cm^2 compared to around 1500 and 2500 pg/cm^2 for Plant A and Plant B, respectively. A strong decrease in ATP concentrations in the fouling layer was observed after chemical cleaning. ATP removal efficiency (which can be regarded as a microbial in-activation efficiency) was relatively high for all the three cases (>70%) with the highest inactivation efficiency of around 100% for Plant A. The TOC results for the three case studies before and after chemical cleaning are shown in Fig. 3b to reveal the amount of organic matter actually removed by cleaning. TOC concentration before cleaning in Plant A (~130 μg/cm^2) was higher than in the MFS (~80 μg/cm^2) and Plant B (~30 μg/cm^2). TOC removal efficiency demonstrates that Plant A has the most difficult biomass to be removed (removal efficiency around 60%) (Fig. 3b). On the other hand, the MFS showed the highest biomass removal (measured

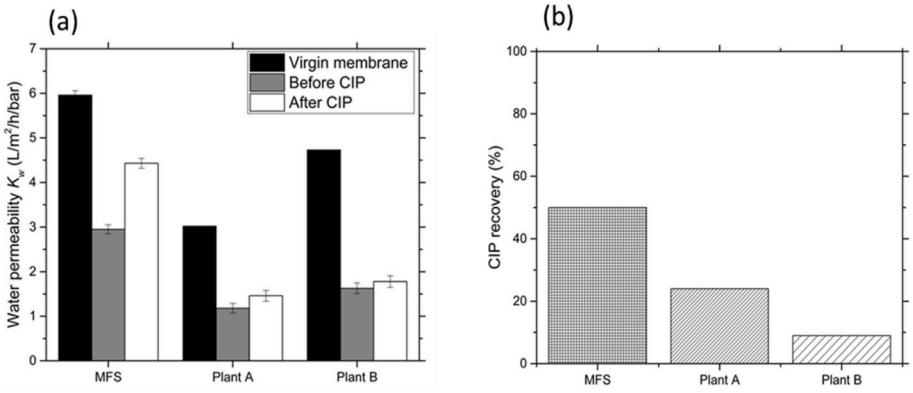

Fig. 2. Water permeability and CIP recovery for the lab-scale MFS and two full-scale modules. a) water permeability for virgin membrane, before and after CIP cleaning, b) CIP efficiency in terms of water permeability recovery (%).

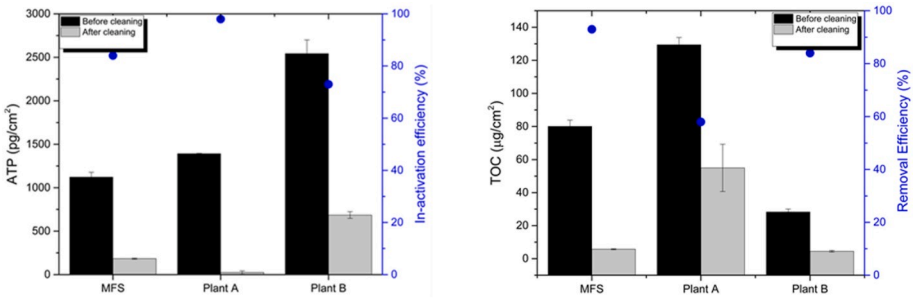

Fig. 3. Accumulated biofilm for the lab-scale MFS and two full-scale modules. a) Adenosine triphosphate concentration (ATP) (pg/cm^2) before and after chemical cleaning; second *Y*-axis in blue shows ATP removal efficiency (inactivation efficiency) by chemical cleaning; b) Total organic carbon concentration (TOC) (µg/cm^2) before and after chemical cleaning; second *Y*-axis in blue shows TOC removal efficiency by chemical cleaning. (For interpretation of the references to color in this figure legend, the reader is referred to the Web version of this article.)

by TOC) and therefore higher cleanability compared to full-scale modules.

3.3. Extracted EPS properties and EPS compositions

The amount of extracted EPS is much higher for full-scale modules (between 20 and 50 µg/cm^2) compared to the lab-scale MFS (~1–3 µg/cm^2) (Table 2). This considerable difference in EPS concentrations between the MFS and full-scale modules is related to the membrane operation time and biofilm age. Interestingly, the protein to polysaccharide ratio (PN/PS) is much lower in MFS compared to the full-scale plants. The PN/PS ratio for MFS, before cleaning, is around 0.5 compared to 2.2 for both Plant A and Plant B, respectively. The results demonstrate that EPS produced in the lab-scale MFS conditions is polysaccharide-rich as opposed to the full-scale EPS which is much more protein-rich (Table 2). The PN/PS ratio after chemical cleaning does not follow any consistent trend in favourability in solubilisation of protein or polysaccharide by the CIP protocols.

3.4. EPS adherence properties and QCM-D measurements

The EPS extracted from the three biofilms demonstrate similar trends in adherence behaviour when they were adsorbed on the QCM-D coated sensors. Milli-Q water was used to measure the baseline of the adsorption experiments. The frequency shift is almost zero during the baseline measurements, followed by the frequency shift of ~3 Hz observed as the background solution was introduced (Fig. 4a). The shift in frequency for the background solution is due to the changes in the solution viscosity and density compared to Milli-Q water. The frequency shift increased as the EPS solution was introduced to the coated sensor. The adsorption of the polymer (EPS) on the coated sensor caused additional frequency changes of ~4 Hz (MFS) and around 8 and 11 Hz for Plant A and B, respectively (Fig. 4a). For the gold (non-coated) sensor, the frequency changes were 2.2 Hz (MFS) and 3.5 and 3.1 Hz (for Plant A and B) (Supplementary Information Fig. S1), indicating only the impact of density and viscosity of the EPS solution. The higher value of frequency shift with EPS solution on coated sensor indicates more deposition (adsorption) of polymer layer on the sensor surface.

Furthermore, the dissipation of energy per oscillation, ΔD, for two overtones (n = 5 and 7) was also measured to analyse adsorbed EPS layer viscoelastic behaviour. The slope of the linear relationship between frequency shift, ΔF, and dissipation change, ΔD, during EPS solution measurement gives an indication of the EPS adsorbed layer fluidity on the coated sensors. The ΔD/ΔF ratio is much higher for the lab-scale EPS around 0.18 compared to Plant A EPS ~0.07 and Plant B around 0.04 (Fig. 4b). The ratio indicates that the adsorbed EPS layer obtained from full-scale samples have higher rigidity (less fluidity properties) compared to lab-scale EPS, as they are adsorbed on the coated sensor.

Table 2
EPS composition of different biofilms from full-scale plants and lab-scale MFS before and after cleaning (n = 3).

EPS composition	Before cleaning			After cleaning		
	MFS	Plant A	Plant B	MFS	Plant A	Plant B
Polysaccharide (µg/cm^2)	1.8	20	6.2	1	4.7	3.4
Protein (µg/cm^2)	0.9	45.6	13.8	0.4	5.2	8.5
Protein/Polysaccharide (PN/PS)	0.5	2.2 ± 0.2	2.2 + 0.3	0.45	1.1 ± 0.1	2.5 ± 0.2

3.5. Optical analysis and SEM imaging

The biofilms covered almost the entire surfaces of the membrane and spacer. SEM images at two magnifications illustrate the biofouling structures for the three case studies. The structures of all three fouling layers appear different (Fig. 5a–c). Specifically, the biofouling layer in

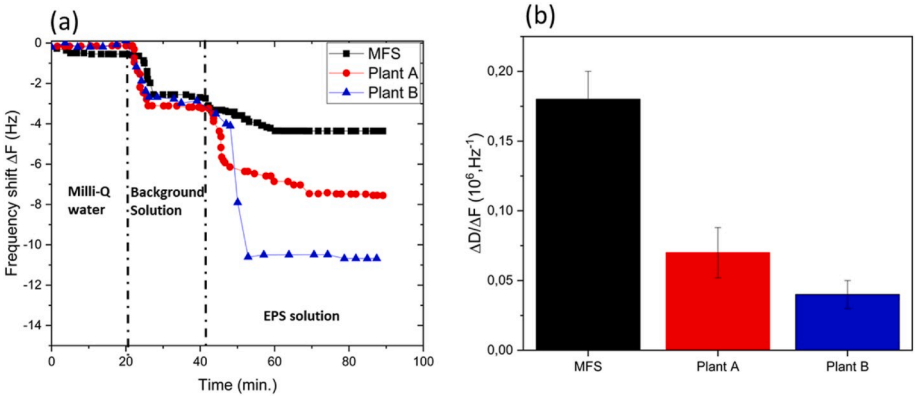

Fig. 4. EPS adherence properties on sensor coated with polyamide using QCM-D; a) the frequency shift (ΔF) showing EPS adherence to the membrane-like surfaces, b) ΔD/ΔF ratio showing EPS fluidity during adsorption to the coated sensors.

the lab-scale MFS at high magnification (Fig. 5d) is more porous than the full-scale biofouling (Fig. 5e and f).

4. Discussion

4.1. CIP efficiency and water permeability

The virgin membrane water permeability in each studied system was reduced significantly due to membrane fouling (Fig. 2a). The water permeability recovery caused by CIP cleaning was greatly different between the lab-MFS and full-scale modules (Fig. 2a). The CIP efficiency was evaluated based on water permeability change caused by CIP cleaning [14]. The applied CIP cleaning had a much higher efficiency on lab-scale MFS (~50%) compared to around 20 and 10% for full-scale modules (Fig. 2b). The reduction in water permeability and water flux due to fouling layer are vastly reported in literature [2,8,14,19,20,39,40]. The observed difference in the CIP efficiency (in terms of flux recovery) could be attributed to the different CIP history and EPS properties of full-scale and lab-scale biofouling layers. Al Ashhab et al. [19] observed that CIP efficiency in flux recovery decreases as the number of CIP events increased. They correlated the reduction in the CIP efficiency after several CIP rounds to the selection of more resilient and adhesive cells and EPS following several CIP events. Recently, Tew et al. [31] reported a significant difference in CIP efficiency when comparing the lab-scale and industrial-scale RO membrane for concentrating milk. They used identical feed water solutions and similar cleaning routines while only the operation time was different (biofouling age). They observed that the chemical cleaning could restore laboratory flux to a high extent (compared to original flux) while the chemical cleanings had little or no impacts on membrane permeability in industrial membranes. The observed differences are attributed to, for example, different lipid type and concentration. In our study, despite considerable biomass removal (Fig. 3), the water flux never fully restored after the CIP events. This confirms previous observations that presence of a thin and dense biofouling layer (i.e., biofilm base layer) would dominate the resistance to water flux and reduce total membrane permeability [41–43].

4.2. Biomass quantification

The biomass quantification results show that ATP and TOC values in this study are in the range of reported data in literature [7]. The ATP concentration in the fouling layer of Plant B is higher than the ones in

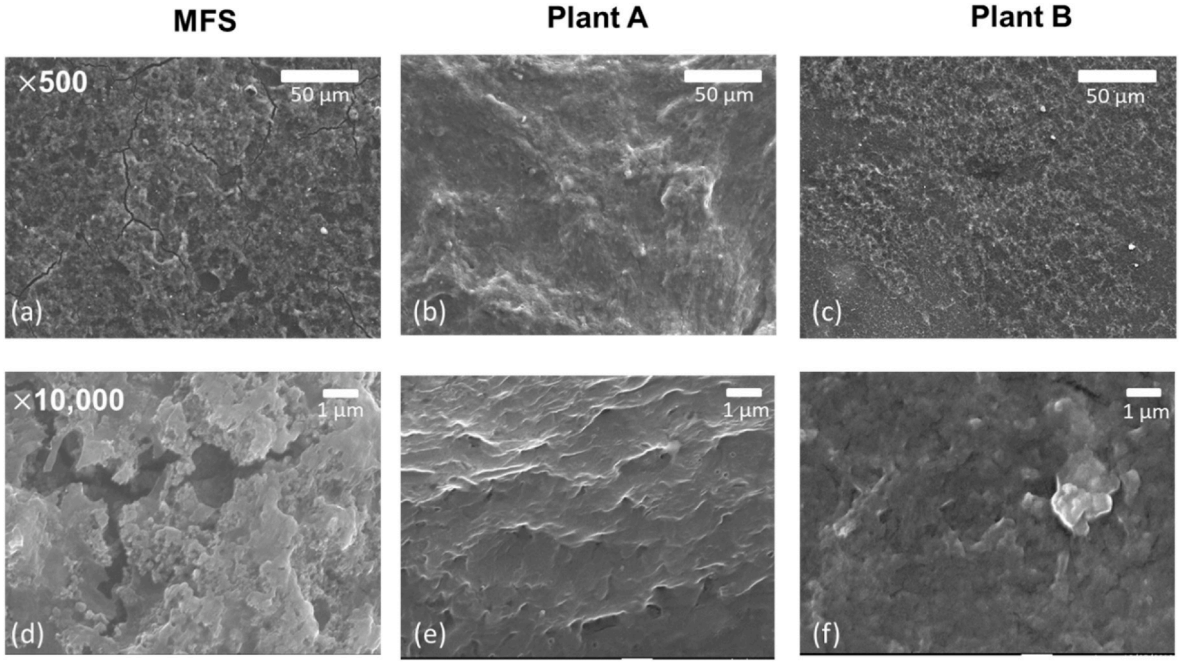

Fig. 5. SEM micrographs of all three biofilm cases, at two zoom levels (500x and 10,000x, upper and lower row respectively).

Plant A and MFS (Fig. 3a), which can be related to the observed algae bloom in the source of the feed water. Algae contribute to an increase in the Natural Organic Matter (NOM) [44] and dissolved organic matter (e.g., EPS) [45] in the feed water. The relative low ATP concentration in Plant A is accompanied with a fairly high TOC concentration (Fig. 3b), which suggests deposition of organic carbon in form of NOM [7] leading to significant reduction to hydraulic permeability [46]. The ATP in-activation and TOC removal efficiencies are also in accordance with reported studies [21,33]. In the current study, high TOC removal was not linked to the low concentration of divalent cations in the fouling layer, as widely reported in literature [6,47]. The MFS has higher TOC removal (compared to full-scale cases) while the concentration of divalent cations is also higher than in the full-scale cases (Table S1). Thus, the higher TOC removal in MFS can be attributed to more porous morphology of the fouling layer in MFS (Fig. 5), which leads to greater EPS solubilisation (due to better cleanant diffusion) and resulting in higher biomass removal. In our study, the average ATP removal was around 83% compared to the average TOC removal of ~76% (higher organic matter compared to cells), in-line with the general observation that TOC removal is lower than ATP removal [21]. Although chemical cleaning mechanisms of biomass removal (e.g., solubilisation, hydrolysis, …) are widely discussed [7,20,48,49], the ATP and TOC removal efficiencies provide limited information on the actual effect of chemical cleaning and the underlying reason for the observed difference in performance parameters (i.e., membrane permeability recovery) [7,21]. Therefore, EPS as a biofilm matrix, which reveals crucial information about biofouling layer composition and adherence was studied in more detail here.

4.3. EPS composition and protein to polysaccharide ratio (PN/PS)

The significant difference in chemical cleaning efficiency between lab-scale MFS and full-scale plants (Fig. 2a and b) could be attributed to the remarkable differences in the protein to polysaccharide ratio (PN/PS) of extracted EPS (Table 2). The lab-grown biofilm consisted of polysaccharide-rich EPS (low PN/PS) that can be correlated to the young biofilm and nutrient excess (typical in lab studies). This is in agreement with other studies reporting the EPS composition for biofilms grown in lab-scale RO systems [16,19]. On the other hand, full-scale plant biofilms in our study consisted of mainly protein-rich EPS (high PN/PS). Herzberg et al. [6] reported polysaccharide-rich EPS for the biofilms grown under lab-scale conditions using a synthetic wastewater. The PN/PS ratio of extracted EPS increased with increasing SRT in MBR. The results suggest PN/PS ratio increases with an increase in biofilm age. In addition, the PN/PS ratio increases as the biofilm age increases during dead-end UF for the biofilms grown under nutrient limitation [29]. The transition from polysaccharide-rich EPS in the young biofilm (low PN/PS) to protein-rich EPS in the mature biofilms (high PN/PS) has been explained by the need to have polysaccharides with high adherence in the initial biofilm development stages, required for structural integrity [28,50,51]. However, Fong et al. [52] reported that not all polysaccharides facilitate biofilm adhesion. Proteins found in EPS are also claimed to contribute importantly to biofilm attachment to the surface and biofilm stabilization [52]. Thus, it seems that different proteins and polysaccharides with different properties (e.g., electrostatic charge) are preferred for biofilm adhesion in the early stages of biofilm formation. Therefore, the literature on EPS characterization and functionality is speculative and uncertain as described above and in more details by Seviour et al. [53]. For instance, the significant role of polysaccharides on biofilm adhesion often referred to work of Christensen [51] despite the fact that the authors clearly stated that their speculations have no “direct and conclusive evidence”.

4.4. EPS adherence properties

The quasi-quantitative results of QCM-D measurements (ΔF and ΔD) allow us to compare adherence properties of lab-scale and full-scale EPS on the coated sensor. The lab-scale EPS exhibited a lower adherence to the sensor surface compared to the full-scale EPS (Fig. 4), which can be correlated to differences in their composition and the number of CIP events performed. Al Ashhab et al. [19] reported that the biofilm adherence to the coated sensor increased only after five rounds of CIP cleaning, due to the selection of specific microbial community with higher adherence to the membrane surface. Moreover, biofilms grown under low substrate concentration have higher adherence to the surface compared to the biofilms grown under nutrient excess (the biofilms had equal age) [54]. This is in agreement with the finding of this study where the full-scale biofilm (nutrient-limited) has higher adherence than lab-scale biofilm (nutrient-excess). The ΔD/ΔF ratio (Fig. 4b) was developed to analyse the rigidity of adsorbed EPS layer on the sensors. The higher fluidity (less rigidity) of EPS from lab-scale MFS with no CIP history compared to full-scale EPS with several rounds of CIP is in accordance with reported results by Al Ashhab et al. [19]. One should note that the QCM-D results are only reliable for the comparison only if the EPS samples are extracted using an identical technique. Moreover, the EPS adsorption measurements should be carried out also on the bare (uncoated) gold sensor to evaluate impacts on EPS solution density and viscosity on the frequency changes (Supplementary Information Fig. S1).

4.5. Practical implications and future research

There have been extensive efforts in the development of novel, cost effective and efficient CIP protocols to reduce fouling impacts in membrane processes. CIP protocols are often optimized in the lab using synthetic feed water and short-term experiments [31]. However, the CIP efficiency is significantly different in laboratory and industrial conditions, which is likely due to considerable difference in biofilm composition [7,31]. This study proposed that the observed differences in CIP efficiency are caused by the difference between the EPS composition in the full-scale and lab-scale membranes. Thus, the CIP protocols should not be developed using synthetic feed water and fouling layer developed over a short period of time. We suggest that a more detailed EPS composition analysis (e.g., by mass spectrometry) could give qualitative valuable information on the protein and polysaccharide fraction of EPS.

The knowledge of EPS could help to choose the optimal CIP protocols. In this sense. we could customize chemical solvents and treatments based on different EPS compositions to maximize solubilisation. For example, some EPS compositions are reported to be much more soluble in acidic conditions, as oppose to the others which are solubilized to a higher degrees in alkaline conditions or in ionic liquids [55].

However, lack of unified EPS extraction and characterization protocols makes comparing the available literature data extremely difficult [53]. The novel EPS extraction and characterization techniques provide an opportunity to develop better CIP protocols by enhancing EPS solubilisation [16]. However, one should also note the limitations of the current EPS extraction and characterization methods [34]. The relatively low EPS extraction yield and the impossibility to distinguish between excreted polymer (produced by microorganism) and deposited polymer (from the feed water) limit further understanding of the EPS role in CIP efficiency. Thus, further research should also focus on developing alternative and reliable EPS extraction and characterization methods [34]. EPS properties in the membrane system should be evaluated in the lab by long-term studies using real wastewater. This would allow to estimate the minimum experimental time required to properly replicate the full-scale membrane biofilms.

5. Conclusions

The goal of this study was to investigate suitability of CIP results from lab-scale fouling experiments for applications in full-scale RO plants. A fouling experiment under lab-conditions (short-term and

synthetic feed water) and two full-scale RO membrane autopsies were carried out. The CIP efficiency measurements as well biomass analysis have been done. The main study findings can be summarized by:

- Chemical cleaning efficiency is much higher for fouled lab-scale MFS than for module full-scale plants.
- Higher CIP efficiency for the lab-scale MFS than the full-scale modules is correlated to a considerable difference in their EPS properties. The extracted lab-scale EPS is polysaccharide-rich while the EPS extracted from full-scale modules mainly consist of protein.
- The EPS extracted from full-scale fouled membranes exhibited higher adherence to the membrane surface compared to the lab-scale EPS.

This study indicates that the lab-scale CIP results are not representative for the full-scale applications. The typical lab-scale fouling experiments (young biofilms which are fed with nutrient excess feed water) are not representative of full-scale conditions. We propose that CIP protocols should be optimized in long-term experiments using the realistic feed water.

Declaration of competing interest

The authors declare that they have no known competing financial interests or personal relationships that could have appeared to influence the work reported in this paper.

CRediT authorship contribution statement

M. Jafari: Investigation, Data curation, Writing - original draft. **A. D'haese:** Investigation. **J. Zlopasa:** Investigation. **E.R. Cornelissen:** Supervision. **J.S. Vrouwenvelder:** Conceptualization. **K. Verbeken:** Resources. **A. Verliefde:** Resources. **M.C.M. van Loosdrecht:** Supervision, Funding acquisition. **C. Picioreanu:** Supervision, Funding acquisition.

Acknowledgements

This study was funded by European Union's Horizon 2020 research and innovation program under the Marie Skłodowska-Curie grant agreement No. 676070. The authors gratefully acknowledge Özgür Gölbasi and David Moed (Evides Industriewater B.V., The Netherlands) and Celestin Claeys (De Watergroep N.V., Belgium) for kindly providing membrane modules and related supports. The authors acknowledge Elien Wallaert (Ghent University) for her great help in proving SEM images. This communication reflects only the authors' view and the Research Executive Agency of the EU is not responsible for any use that may be made of the information it contains.

Appendix A. Supplementary data

Supplementary data to this article can be found online at https://doi.org/10.1016/j.memsci.2020.118189.

References

[1] H.C. Flemming, Biofouling in water systems – cases, causes and countermeasures, Appl. Microbiol. Biotechnol. 59 (2002) 629–640.
[2] J.S. Vrouwenvelder, S.A. Manolarakis, J.P. van der Hoek, J.A. van Paassen, W. G. van der Meer, J.M. van Agtmaal, H.D. Prummel, J.C. Kruithof, M.C. van Loosdrecht, Quantitative biofouling diagnosis in full scale nanofiltration and reverse osmosis installations, Water Res. 42 (2008) 4856–4868.
[3] C. Dreszer, J.S. Vrouwenvelder, A.H. Paulitsch-Fuchs, A. Zwijnenburg, J. C. Kruithof, H.C. Flemming, Hydraulic resistance of biofilms, J. Membr. Sci. 429 (2013) 436–447.
[4] K.J. Martin, D. Bolster, N. Derlon, E. Morgenroth, R. Nerenberg, Effect of fouling layer spatial distribution on permeate flux: a theoretical and experimental study, J. Membr. Sci. 471 (2014) 130–137.
[5] E. Huertas, M. Herzberg, G. Oron, M. Elimelech, Influence of biofouling on boron removal by nanofiltration and reverse osmosis membranes, J. Membr. Sci. 318 (2008) 264–270.
[6] M. Herzberg, S. Kang, M. Elimelech, Role of extracellular polymeric substances (EPS) in biofouling of reverse osmosis membranes, Environ. Sci. Technol. 43 (2009) 4393–4398.
[7] F. Beyer, B.M. Rietman, A. Zwijnenburg, P. van den Brink, J.S. Vrouwenvelder, M. Jarzembowska, J. Laurinonyte, A.J.M. Stams, C.M. Plugge, Long-term performance and fouling analysis of full-scale direct nanofiltration (NF) installations treating anoxic groundwater, J. Membr. Sci. 468 (2014) 339–348.
[8] N.M. Farhat, L. Javier, M.C.M. Van Loosdrecht, J.C. Kruithof, J.S. Vrouwenvelder, Role of feed water biodegradable substrate concentration on biofouling: biofilm characteristics, membrane performance and cleanability, Water Res. 150 (2019) 1–11.
[9] O.D. Basu, Backwashing, in: E. Drioli, L. Giorno (Eds.), Encyclopedia of Membranes, Springer Berlin Heidelberg, Berlin, Heidelberg, 2015, pp. 1–3.
[10] J.S. Vrouwenvelder, J. Buiter, M. Riviere, W.G.J. van der Meer, M.C.M. van Loosdrecht, J.C. Kruithof, Impact of flow regime on pressure drop increase and biomass accumulation and morphology in membrane systems, Water Res. 44 (2010) 689–702.
[11] Y. Wibisono, K.E. El Obied, E.R. Cornelissen, A.J.B. Kemperman, K. Nijmeijer, Biofouling removal in spiral-wound nanofiltration elements using two-phase flow cleaning, J. Membr. Sci. 475 (2015) 131–146.
[12] E.R. Cornelissen, J.S. Vrouwenvelder, S.G.J. Heijman, X.D. Viallefont, D. Van Der Kooij, L.P. Wessels, Periodic air/water cleaning for control of biofouling in spiral wound membrane elements, J. Membr. Sci. 287 (2007) 94–101.
[13] X. Shi, G. Tal, N.P. Hankins, V. Gitis, Fouling and cleaning of ultrafiltration membranes: a review, J Water Process Eng 1 (2014) 121–138.
[14] S. Madaeni, Y. Mansourpanah, Chemical cleaning of reverse osmosis membranes fouled by whey, Desalination 161 (2004) 13–24.
[15] F. Beyer, J. Laurinonyte, A. Zwijnenburg, A.J.M. Stams, C.M. Plugge, Membrane fouling and chemical cleaning in three full-scale reverse osmosis plants producing demineralized water, J. Eng. (2017) 1–14, 2017.
[16] H. Sanawar, I. Pinel, N.M. Farhat, S.S. Bucs, J. Zlopasa, J.C. Kruithof, G. J. Witkamp, M.C.M. van Loosdrecht, J.S. Vrouwenvelder, Enhanced biofilm solubilization by urea in reverse osmosis membrane systems, Water Res. 1 (2018).
[17] L.A. Bereschenko, H. Prummel, G.J. Euverink, A.J. Stams, M.C. van Loosdrecht, Effect of conventional chemical treatment on the microbial population in a biofouling layer of reverse osmosis systems, Water Res. 45 (2011) 405–416.
[18] L.A. Bereschenko, A.J.M. Stams, G.J.W. Euverink, M.C.M. van Loosdrecht, biofilm formation on reverse osmosis membranes is initiated and dominated by, Appl. Microbiol. Biotechnol. 76 (2010) 2623–2632.
[19] A. Al Ashhab, A. Sweity, B. Bayramoglu, M. Herzberg, O. Gillor, Biofouling of reverse osmosis membranes: effects of cleaning on biofilm microbial communities, membrane performance, and adherence of extracellular polymeric substances, Biofouling 33 (2017) 397–409.
[20] N. Porcelli, S. Judd, Chemical cleaning of potable water membranes: a review, Separ. Purif. Technol. 71 (2010) 137–143.
[21] W.A. Hijnen, C. Castillo, A.H. Brouwer-Hanzens, D.J. Harmsen, E.R. Cornelissen, D. van der Kooij, Quantitative assessment of the efficacy of spiral-wound membrane cleaning procedures to remove biofilms, Water Res. 46 (2012) 6369–6381.
[22] S.S. Bucs, R. Valladares Linares, J.O. Marston, A.I. Radu, J.S. Vrouwenvelder, C. Picioreanu, Experimental and numerical characterization of the water flow in spacer-filled channels of spiral-wound membranes, Water Res. 87 (2015) 299–310.
[23] S.A. Creber, J.S. Vrouwenvelder, M.C.M. van Loosdrecht, M.L. Johns, Chemical cleaning of biofouling in reverse osmosis membranes evaluated using magnetic resonance imaging, J. Membr. Sci. 362 (2010) 202–210.
[24] D.J. Miller, P.A. Araujo, P.B. Correia, M.M. Ramsey, J.C. Kruithof, M.C. van Loosdrecht, B.D. Freeman, D.R. Paul, M. Whiteley, J.S. Vrouwenvelder, Short-term adhesion and long-term biofouling testing of polydopamine and poly(ethylene glycol) surface modifications of membranes and feed spacers for biofouling control, Water Res. 46 (2012) 3737–3753.
[25] H. Sanawar, A. Siddiqui, S.S. Bucs, N.M. Farhat, M.C.M. van Loosdrecht, J. C. Kruithof, J.S. Vrouwenvelder, Applicability of short-term accelerated biofouling studies to predict long-term biofouling accumulation in reverse osmosis membrane systems, Desalin Water Treat 97 (2017) 72–78.
[26] W.A. Hijnen, E.R. Cornelissen, D. van der Kooij, Threshold concentrations of biomass and iron for pressure drop increase in spiral-wound membrane elements, Water Res. 45 (2011) 1607–1616.
[27] J.S. Vrouwenvelder, J.A.M. van Paassen, L.P. Wessels, A.F. van Dam, S.M. Bakker, The Membrane Fouling Simulator: a practical tool for fouling prediction and control, J. Membr. Sci. 281 (2006) 316–324.
[28] A. Sweity, W. Ying, M.S. Ali-Shtayeh, F. Yang, A. Bick, G. Oron, M. Herzberg, Relation between EPS adherence, viscoelastic properties, and MBR operation: biofouling study with QCM-D, Water Res. 45 (2011) 6430–6440.
[29] P. Desmond, J.P. Best, E. Morgenroth, N. Derlon, Linking composition of extracellular polymeric substances (EPS) to the physical structure and hydraulic resistance of membrane biofilms, Water Res. 132 (2018) 211–221.
[30] S. Bucs, R. Valladares Linares, A. Siddiqui, A. Matin, Z. Khan, M.C.M. van Loosdrecht, R. Yang, M. Wang, K.K. Gleason, J.C. Kruithof, J.S. Vrouwenvelder, Coating of reverse osmosis membranes with amphiphilic copolymers for biofouling control, Desalin Water Treat 68 (2017) 11.
[31] X.W. Tew, S.J. Fraser-Miller, K.C. Gordon, K.R. Morison, A comparison between laboratory and industrial fouling of reverse osmosis membranes used to concentrate milk, Food Bioprod. Process. 114 (2019) 113–121.

[32] J.S. Vrouwenvelder, C. Hinrichs, W.G.J. Van der Meer, M.C.M. Van Loosdrecht, J. C. Kruithof, Pressure drop increase by biofilm accumulation in spiral wound RO and NF membrane systems: role of substrate concentration, flow velocity, substrate load and flow direction, Biofouling 25 (2009) 543–555.
[33] W.A.M. Hijnen, E.R. Cornelissen, D. van der Kooij, Threshold concentrations of biomass and iron for pressure drop increase in spiral-wound membrane elements, Water Res. 45 (2011) 1607–1616.
[34] S. Felz, P. Vermeulen, M.C.M. van Loosdrecht, Y.M. Lin, Chemical characterization methods for the analysis of structural extracellular polymeric substances (EPS), Water Res. 157 (2019) 201–208.
[35] M. DuBois, K.A. Gilles, J.K. Hamilton, P.A. Rebers, F. Smith, Colorimetric method for determination of sugars and related substances, Anal. Chem. 28 (1956) 350–356.
[36] M.M. Bradford, A rapid and sensitive method for the quantitation of microgram quantities of protein utilizing the principle of protein-dye binding, Anal. Biochem. 72 (1976) 248–254.
[37] K.D. Kwon, H. Green, P. Bjöörn, J.D. Kubicki, Model bacterial extracellular polysaccharide adsorption onto silica and Alumina: Quartz crystal microbalance with dissipation monitoring of dextran adsorption, Environ. Sci. Technol. 40 (2006) 7739–7744.
[38] S.-J. Kim, B.S. Oh, H.-W. Yu, L.H. Kim, C.-M. Kim, E.-T. Yang, M.S. Shin, A. Jang, M.H. Hwang, I.S. Kim, Foulant characterization and distribution in spiral wound reverse osmosis membranes from different pressure vessels, Desalination 370 (2015) 44–52.
[39] I.S. Kim, N. Jang, The effect of calcium on the membrane biofouling in the membrane bioreactor (MBR), Water Res. 40 (2006) 2756–2764.
[40] N. Porcelli, S. Judd, Chemical cleaning of potable water membranes: the cost benefit of optimisation, Water Res. 44 (2010) 1389–1398.
[41] M. Jafari, N. Derlon, P. Desmond, M.C.M. van Loosdrecht, E. Morgenroth, C. Picioreanu, Biofilm compressibility in ultrafiltration: a relation between biofilm morphology, mechanics and hydraulic resistance, Water Res. 157 (2019) 335–345.
[42] M. Jafari, P. Desmond, M.C.M. van Loosdrecht, N. Derlon, E. Morgenroth, C. Picioreanu, Effect of biofilm structural deformation on hydraulic resistance during ultrafiltration: a numerical and experimental study, Water Res. 145 (2018) 375–387.
[43] N. Derlon, A. Grutter, F. Brandenberger, A. Sutter, U. Kuhlicke, T.R. Neu, E. Morgenroth, The composition and compression of biofilms developed on ultrafiltration membranes determine hydraulic biofilm resistance, Water Res. 102 (2016) 63–72.
[44] N. Her, G. Amy, H.-R. Park, M. Song, Characterizing algogenic organic matter (AOM) and evaluating associated NF membrane fouling, Water Res. 38 (2004) 1427–1438.
[45] J.B. Castaing, A. Massé, V. Séchet, N.E. Sabiri, M. Pontié, J. Haure, P. Jaouen, Immersed hollow fibres microfiltration (MF) for removing undesirable micro-algae and protecting semi-closed aquaculture basins, Desalination 276 (2011) 386–396.
[46] D. Violleau, H. Essis-Tome, H. Habarou, J.P. Croud, M. Pontie, Fouling studies of a polyamide nanofiltration membrane by selected natural organic matter: an analytical approach, Desalination 173 (2005) 223–238.
[47] Q. Li, M. Elimelech, Organic fouling and chemical cleaning of nanofiltration Membranes: measurements and mechanisms, Environ. Sci. Technol. 38 (2004) 4683–4693.
[48] G. Trägårdh, Membrane cleaning, Desalination 71 (1989) 325–335.
[49] S.S. Madaeni, Y. Mansourpanah, Chemical cleaning of reverse osmosis membranes fouled by whey, Desalination 161 (2004) 13–24.
[50] D.H. Limoli, C.J. Jones, D.J. Wozniak, Bacterial extracellular polysaccharides in biofilm formation and function, Microbiol. Spectr. 3 (2015).
[51] B.E. Christensen, The role of extracellular polysaccharides in biofilms, J. Biotechnol. 10 (1989) 181–202.
[52] J.N.C. Fong, F.H. Yildiz, Biofilm matrix proteins, Microbiol. Spectr. 3 (2015), https://doi.org/10.1128/microbiolspec.MB-0004-2014.
[53] T. Seviour, N. Derlon, M.S. Dueholm, H.-C. Flemming, E. Girbal-Neuhauser, H. Horn, S. Kjelleberg, M.C.M. van Loosdrecht, T. Lotti, M.F. Malpei, R. Nerenberg, T.R. Neu, E. Paul, H. Yu, Y. Lin, Extracellular polymeric substances of biofilms: suffering from an identity crisis, Water Res. 151 (2019) 1–7.
[54] A. Allen, O. Habimana, E. Casey, The effects of extrinsic factors on the structural and mechanical properties of Pseudomonas fluorescens biofilms: a combined study of nutrient concentrations and shear conditions, Colloids Surf., B 165 (2018) 127–134.
[55] M. Boleij, T. Seviour, L.L. Wong, M.C.M. van Loosdrecht, Y. Lin, Solubilization and characterization of extracellular proteins from anammox granular sludge, Water Res. 164 (2019), 114952.